Single Joint Control of a Flexible Industrial Manipulator using \mathcal{H}_{∞} Loop Shaping

Patrik Axelsson, Anders Helmersson, Mikael Norrlöf

Division of Automatic Control

E-mail: axelsson@isy.liu.se, andersh@isy.liu.se, mino@isy.liu.se

26th October 2012

Report no.: LiTH-ISY-R-3053

Submitted to European Control Conference 2013

Address:

Department of Electrical Engineering Linköpings universitet SE-581 83 Linköping, Sweden

WWW: http://www.control.isy.liu.se



Abstract

Control of a flexible joint of an industrial manipulator using \mathcal{H}_{∞} loop shaping design is presented. Two controllers are proposed; 1) \mathcal{H}_{∞} loop shaping using the actuator position, and 2) \mathcal{H}_{∞} loop shaping using the actuator position and the acceleration of end-effector. The two controllers are compared to a standard PID controller where only the actuator position is measured. Using the acceleration of the end-effector improves the nominal performance. The performance of the proposed controllers is not significantly decreased in the case of model error consisting of an increased time delay or a gain error.

Keywords: Industrial robots, flexible joint, robust control, \mathcal{H}_{∞} loop shaping

Single Joint Control of a Flexible Industrial Manipulator using \mathcal{H}_{∞} Loop Shaping

Patrik Axelsson, Anders Helmersson, and Mikael Norrlöf

Abstract—Control of a flexible joint of an industrial manipulator using \mathcal{H}_{∞} loop shaping design is presented. Two controllers are proposed; 1) \mathcal{H}_{∞} loop shaping using the actuator position, and 2) \mathcal{H}_{∞} loop shaping using the actuator position and the acceleration of end-effector. The two controllers are compared to a standard PID controller where only the actuator position is measured. Using the acceleration of the end-effector improves the nominal performance. The performance of the proposed controllers is not significantly decreased in the case of model error consisting of an increased time delay or a gain error.

I. INTRODUCTION

The requirements for a controller in a modern industrial manipulator is that it should provide high performance, at the same time, robustness to model uncertainty. In the typical standard control configuration for industrial manipulators the actuator positions is the only measurements used in the higher level control loop. At a lower level, in the drive system, the currents and voltages in the motor are measured to provide torque control for the motors. As a result of the development of cost efficient manipulators the mechanical structure has become less rigid, therefore the need for new control structures have emerged [3]. To support the proposed control structures it is necessary to introduce new sensors such as encoders, measuring joint position after the gearbox, and accelerometers, measuring the end-effector acceleration.

Control of robots has been considered for many years. The different contributions differ in e.g. model complexity (actuator dynamics, rigid and flexible joints and links), and control structure (PID, feedback linearization, linear and nonlinear \mathcal{H}_{∞} , sliding mode), as discussed in the survey [12].

Controller synthesis using \mathcal{H}_{∞} methods has been proposed in [15], [16], where the complete nonlinear robot model first is linearised using exact linearization, second a \mathcal{H}_{∞} controller is designed using the linearised model. The remaining nonlinearities due to model errors are seen as uncertainties and/or disturbances. In both papers, the model is rigid and the \mathcal{H}_{∞} controller, using only joint positions, is designed using the mixed-sensitivity method. In [13] \mathcal{H}_{∞} loop shaping with measurements of the actuator positions is applied to a robot. The authors use a flexible joint model which has been linearised. The linearised model makes it possible to use decentralised control, hence \mathcal{H}_{∞} loop shaping is applied to n SISO-systems instead of the complete MIMO-system.

*This work was supported by the Vinnova Excellence Center LINK-SIC. P. Axelsson, A. Helmersson and M. Norrlöf are with Division of Automatic Control, Department of Electrical Engineering, Linköping University, SE-581 83 Linköping, Sweden, {axelsson, andersh, mino}@isy.liu.se.

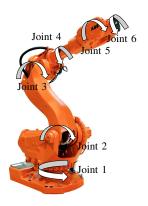


Fig. 1. The 6 DOF industrial manipulator ABB IRB6600, where the joints are indicated by the arrows.

Explicit use of acceleration measurements for control in robotic applications has been reported in, for example, [5], [4], [7], [10] and [17]. In [5], a control law using motor position and acceleration of the load in the feedback loop is proposed for a Cartesian robot¹. The robot is assumed to be flexible and modelled as a two-mass system, where the masses are connected by a linear spring-damper pair. Another control law of a Cartesian robot using acceleration measurements is presented in [4]. The model is a rigid joint model and the evaluation is made both in simulation and experiments.

In [7] a 2 degrees-of-freedom (DOF) manipulator is controlled using acceleration measurements of the end-effector. The model is assumed to be rigid and it is exactly linearised. The joint angular acceleration used in the nonlinear feedback loop is calculated using the inverse forward kinematic acceleration model and the measured acceleration. The use of direct measurements of the angular acceleration in the feedback loop is presented in [10] for both rigid and flexible joint models. A more recent work is presented in [17], where a 3 DOF manipulator is controlled using only measurements of the end-effector acceleration.

This contribution investigates the possibility to use both \mathcal{H}_{∞} loop shaping [8] and measurements of the end-effector acceleration. The controllers are synthesised for a highly flexible single joint model. The joint model represents the first joint of a serial 6 DOF industrial manipulator, see Figure 1. Compared to many previous contributions, the flexible joint model is not a two-mass model, but instead described by a

¹For a Cartesian robot the joint acceleration is measured directly by an accelerometer, while for a serial type robot there is a non-linear mapping depending on the states.

four-mass model, which is a more representative description of the behaviour of the manipulator [9].

The theory for synthesis of \mathcal{H}_{∞} controllers is presented in Section II, including a brief description of model order reduction. The model describing the robot joint is explained in Section III. In Section IV, the requirements of the system as well as the design of two controllers are described. Finally, Section V shows the simulation results and Section VI concludes the work.

II. CONTROL THEORY

In this section, the general \mathcal{H}_{∞} synthesis design is presented together with an introduction to loop shaping using \mathcal{H}_{∞} methods. At the end, a brief presentation of model order reduction is given.

A. \mathcal{H}_{∞} Control

For design of \mathcal{H}_{∞} controllers the system

$$\begin{pmatrix} z \\ y \end{pmatrix} = \begin{pmatrix} P_{11}(s) & P_{12}(s) \\ P_{21}(s) & P_{22}(s) \end{pmatrix} \begin{pmatrix} w \\ u \end{pmatrix} = P(s) \begin{pmatrix} w \\ u \end{pmatrix}$$
(1)

is considered, where w is the exogenous input signals (disturbances and references), u is the control signal, y is the measurements and z is the exogenous output signals. Using a controller u=K(s)y, see Figure 2(a), the system from w to z can be written as

$$z = F_l(P, K)w, (2)$$

where $F_l(P,K)$ denotes the lower linear fractional transformation (LFT). The \mathcal{H}_{∞} controller is the controller that minimises

$$||F_l(P,K)||_{\infty} = \max_{\omega} \bar{\sigma} \left(F_l(P,K)(i\omega) \right), \tag{3}$$

where $\bar{\sigma}(\cdot)$ denotes the maximal singular value. It is not always necessary and sometimes not even possible to find the optimal \mathcal{H}_{∞} controller. Instead, a suboptimal controller is derived such that

$$||F_l(P,K)||_{\infty} < \gamma, \tag{4}$$

where γ can be reduced iteratively until a satisfactory controller is obtained. Often the aim is to get $\gamma \approx 1$. Efficient iterative algorithms to find K(s), such that (4) is fulfilled, exist, see e.g. [14], [18], where two Riccati equations are solved in general. Note that the resulting \mathcal{H}_{∞} -controller has the same state dimension as P. A stabilising proper controller exists if a number of assumptions are fulfilled as discussed in [14].

B. Loop Shaping using \mathcal{H}_{∞} Synthesis

In this paper, loop shaping using \mathcal{H}_{∞} synthesis is considered. The method was first presented in [8] and is based on robust stabilisation of a normalised coprime factorisation of the system as described in [6]. Let the system G be described by its left coprime factorisation $G = M^{-1}N$, where M and N are stable transfer functions. The set of perturbed plants

$$G_p = \left\{ (M + \Delta_M)^{-1} (N + \Delta_N) : \left\| \begin{pmatrix} \Delta_N & \Delta_M \end{pmatrix} \right\|_{\infty} < \frac{1}{\gamma} \right\},\,$$

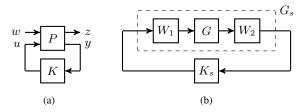


Fig. 2. System description for general \mathcal{H}_{∞} synthesis (a) and loop shaping (b).

where Δ_M , and Δ_N are stable unknown transfer functions representing the uncertainties, is robustly stabilised by the controller K(s) if the nominal feedback system is stable and [6]

$$\left\| \begin{pmatrix} K \\ I \end{pmatrix} (I - GK)^{-1} M^{-1} \right\|_{\infty} \le \gamma. \tag{5}$$

Synthesis of the controller K consists of the solution of two algebraic Riccati equations and does not involve any iteration of γ , see [6] for more details.

For loop shaping [8], the system G(s) is pre- and postmultiplied with weights $W_1(s)$ and $W_2(s)$, see Figure 2(b), such that the shaped system $G_s(s) = W_2(s)G(s)W_1(s)$ has the desired properties. The controller $K_s(s)$ is then obtained using the method described above applied on the system $G_s(s)$. Finally, the controller K(s) is given by

$$K(s) = W_1(s)K_s(s)W_2(s).$$
 (6)

Note that the structure in Figure 2(b) for loop shaping can be rewritten as a standard \mathcal{H}_{∞} problem according to Figure 2(a), see [18] for details.

The MATLAB function ncfsyn, included in the Robust Control Toolbox, is used in this paper for synthesis of \mathcal{H}_{∞} controllers using loop shaping.

C. Model Order Reduction

Controllers that are synthesised using \mathcal{H}_{∞} design methods often get a high model order. The total model order for an \mathcal{H}_{∞} design is the sum of the order of the system and the order of all the weights introduced in the design process. For implementation aspects, it is preferable to have a low order controller. It can therefore be advantages to analyse if the order of the controller can be reduced without changing the behaviour of the controller.

Before the model is reduced, a balanced realisation is derived such that the controllability and observability Gramians $\mathcal C$ and $\mathcal O$ satisfy

$$C = \mathcal{O} = \operatorname{diag}(\sigma_1, \dots, \sigma_n) = \Sigma,$$
 (7)

where $\sigma_1 \ge ... \ge \sigma_n > 0$ are the Hankel singular values. The balanced model is then partitioned according to

$$A = \begin{pmatrix} A_{11} & A_{12} \\ A_{21} & A_{22} \end{pmatrix}, B = \begin{pmatrix} B_1 \\ B_2 \end{pmatrix}, \tag{8}$$

$$C = \begin{pmatrix} C_1 & C_2 \end{pmatrix}, \ \Sigma = \begin{pmatrix} \Sigma_1 & 0 \\ 0 & \Sigma_2 \end{pmatrix},$$
 (9)

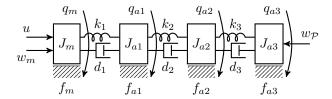


Fig. 3. A four-mass flexible joint model, where J_m is the motor and J_{a1} , J_{a2} , and J_{a3} are the arm divided up in three parts.

where the diagonal elements in Σ_2 are small enough compared to the values in Σ_1 , meaning that the model is not affected if the lower part of the system is removed. The model can be reduced in two ways; i) Truncation, where the reduced model is given by (A_{11}, B_1, C_1, D) and ii) Residualization. A more throughout description is given in [14].

Note that there is no guarantee that the resulting, reduced controller, stabilises the system. To guarantee the stability, special methods for synthesis of low order controllers must be used.

III. ROBOT MODEL

The model considered in this paper is a four-mass model of a single flexible joint, see Figure 3, presented in [9]. The model corresponds to joint 1 of a serial 6 DOF industrial manipulator, see Figure 1, and the model parameters are computed using system identification of experimental data.

Input to the system is the motor torque u, the motor disturbance w_m and the tool disturbance $w_{\mathcal{P}}$. The four masses are connected by spring-damper pairs, where the first mass corresponds to the motor. The other masses are placed along the arm. The first spring-damper pair is modelled by a linear damper and nonlinear spring, whereas the other springdamper pairs are modelled as linear springs. The non-linear spring is characterised by a low stiffness for low torques and a high stiffness for high torques. This behaviour is typical for compact gear boxes, such as harmonic drive [11]. For design of the \mathcal{H}_{∞} controllers, the nonlinear model is linearised in the high stiffness region, meaning that a constant torque, e.g. gravity, is acting on the joint. Moreover, the friction torques are assumed to be linear and the input torque u is limited to ± 20 Nm. The output of the system is the motor position q_m and the tool acceleration $\hat{\mathcal{P}}$, where

$$\mathcal{P} = \frac{l_1 q_{a1} + l_2 q_{a2} + l_3 q_{a3}}{\eta}.$$
 (10)

In (10), η is the gear ratio and l_1 , l_2 , and l_3 are the respective link lengths.

The flexible joint model can be described by a set of four ODEs according to

$$J_{m}\ddot{q}_{m} = u + w_{m} - f_{m}\dot{q}_{m}$$

$$-k_{1}(q_{m} - q_{a1}) - d_{1}(\dot{q}_{m} - \dot{q}_{a1}), \qquad (11a)$$

$$J_{a1}\ddot{q}_{a1} = -f_{a1}\dot{q}_{a1} + k_{1}(q_{m} - q_{a1}) + d_{1}(\dot{q}_{m} - \dot{q}_{a1})$$

$$-k_{2}(q_{a1} - q_{a2}) - d_{2}(\dot{q}_{a1} - \dot{q}_{a2}), \qquad (11b)$$

$$J_{a2}\ddot{q}_{a2} = -f_{a2}\dot{q}_{a2} + k_2(q_{a1} - q_{a2}) + d_1(\dot{q}_{a1} - \dot{q}_{a2}) - k_3(q_{a2} - q_{a3}) - d_3(\dot{q}_{a2} - \dot{q}_{a3}),$$
(11c)
$$J_{a3}\ddot{q}_{a3} = w_{\mathcal{P}} - f_{a3}\dot{q}_{a3}$$

$$+k_3(q_{a2}-q_{a3})+d_3(\dot{q}_{a2}-\dot{q}_{a3}).$$
 (11d)

From the set of ODEs (11), a linear state space model can be derived according to

$$\dot{x} = Ax + Bu + B_w w \tag{12a}$$

$$y = Cx + Du + D_w w ag{12b}$$

where

$$w = \begin{pmatrix} w_m & w_{\mathcal{P}} \end{pmatrix}^{\mathsf{T}},\tag{13a}$$

$$x = (q_m \quad q_{a1} \quad q_{a2} \quad q_{a3} \quad \dot{q}_m \quad \dot{q}_{a1} \quad \dot{q}_{a2} \quad \dot{q}_{a3})^\mathsf{T},$$
 (13b)

which is used for synthesis of the \mathcal{H}_{∞} controllers. Note that the matrix C differs for the different controllers.

IV. DESIGN OF CONTROLLERS

In this section, two controllers based on loop shaping using \mathcal{H}_{∞} synthesis are presented. The first controller uses only the motor angle q_m as measurement, whereas the second controller uses both q_m and the acceleration of the tool $\ddot{\mathcal{P}}$ as measurements. The two controllers are compared to an ordinary PID controller where only q_m is measured. The PID controller is tuned to give the same performance as the best controller presented in [9].

A. Requirements

The controllers using \mathcal{H}_{∞} loop shaping are designed to give better performance than the PID controller. In practise it means that the \mathcal{H}_{∞} controllers should attenuate the disturbances at least as much as the PID controller and the cut-off frequency should be approximately the same.

In Figure 4, the singular values of the two systems from w to $y=q_m$ and w to $y=\left(q_m\ \ddot{\mathcal{P}}\right)^\mathsf{T}$ show that an integrator is present. It means that in order to attenuate the disturbances, it is required to have at least two integrators in the open loop GK. Since G already has one integrator, see Figure 4, the other integrator has to be included in the controller K. An integrator is included in the controller if W_1 or W_2 has one integrator, recall (6).

In addition to nominal performance, the robustness of the controllers with respect to increased time delay and increased system gain is investigated. An increase in the time delay makes the system lose phase, hence a to small phase margin ϕ_m for a SISO-system can make the closed-loop system unstable if the time delay increases. The requirement for a stable closed-loop system is to have $\phi_m > \omega_c T$, where ω_c is the cut-off frequency and T the total time delay. If instead the gain of the open-loop system increases, the closed-loop system can be unstable if the gain margin is not large enough. Note that phase and gain margins has no trivial analogy in the case of MIMO-systems. The requirements for the controllers in this paper are to handle a 4 times higher time delay and a gain increase of 2.5.

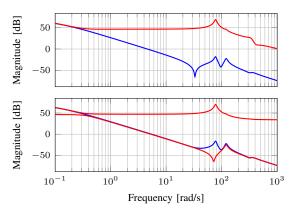


Fig. 4. Singular values for the system from u to y (top) and w to y (bottom), for $y=q_m$ (blue) and $y=(q_m\ \ddot{\mathcal{P}})^{\mathsf{T}}$ (red).

B. Choice of Weights

1) Loop Shaping using q_m : Using only q_m as a measurement gives a SISO-system, hence W_1 and W_2 are scalar transfer functions. Since it is a linear SISO-system it does not matter which one of W_1 and W_2 that is considered since the transfer functions commute with the system G(s). Therefore, $W_1(s)=1$ and $W_2(s)$ is chosen such that the desired loop shape is obtained. First of all, it is necessary to have an integrator in W_2 to be able to handle the disturbances at low frequencies. Having a pure integrator will lead to that the phase margin will be decreased, a zero in s=-10 is therefore added in order not to change the loop gain for frequencies above $10 \, \mathrm{rad/s}$. The gain is then increased until the cut-off frequency is the desired one. The loop shape have peaks above $30 \, \mathrm{rad/s}$. To reduce the magnitude of the peaks a modified elliptic filter

$$H(s) = \frac{0.5227s^2 + 3.266s + 1406}{s^2 + 5.808s + 2324}$$
 (14)

is introduced in W_2 . The filter H(s) has a gain of approximately $0\,\mathrm{dB}$ up to the frequency $50\,\mathrm{rad/s}$, after that it drops down to approximately $-10\,\mathrm{dB}$. Ripple which is unavoidable is present in both the pass and stop band. The weights are finally given as

$$W_1(s) = 1, \quad W_2(s) = 100 \frac{s+10}{s} H(s).$$
 (15)

Using ncfsyn a controller of order 13 is obtained where $\gamma=2.3$, hence the maximum stability margin is $\|(\Delta_N - \Delta_M)\|_{\infty} < 0.43$. The resulting loop gain is shown in Figure 5. Also, the loop gain using the PID controller is presented. In Figure 6, the magnitude of the two controllers are presented. The PID controller is smoother than the other controller. The reason is that a part of the system dynamics is included in the controller when loop shaping synthesis is performed. It tries to remove the resonance peaks from the system, which can be seen Figure 4, hence the peaks in the amplitude function of the controller. The controller will from now on be denoted by $\mathcal{H}_{\infty}(q_m)$.

2) Loop Shaping using q_m and $\ddot{\mathcal{P}}$: Adding an extra measurement signal in terms of the acceleration of the tool

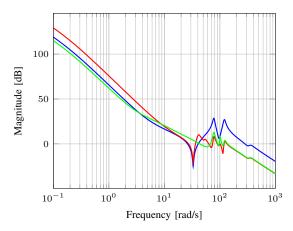


Fig. 5. Loop gain |KG| for PID (blue), $\mathcal{H}_{\infty}(q_m)$ (red) and $\mathcal{H}_{\infty}(q_m, \ddot{\mathcal{P}})$ (green).

gives a system with one input and two outputs. It is now more tricky to shape the loop gain. To start with, it is not possible to have an integrator for both of the measurements. Therefore, the integrator is placed in the channel for q_m since the accelerometer measurement has low frequency noise, such as drift. For the same reason as for the other controller, a zero in s=-3 is introduced. The transfer function from input torque to acceleration of the tool has a high gain in the frequency range of interest. To decrease the gain such that it is comparable with the motor angle measurement, a low pass filter is added in the acceleration channel. The weights are chosen as

$$W_1(s) = 50, \quad W_2(s) = \operatorname{diag}\left(\frac{s+3}{s}, \frac{0.2}{(s+5)^2}\right), \quad (16)$$

giving a controller of order 13 with $\gamma=2.8$ which give a maximum stability margin of $\|(\Delta_N - \Delta_M)\|_{\infty} < 0.36$. The resulting loop gain is shown in Figure 5, where it can be seen that there are peaks present above the cut-off frequency. In the case with only q_m as a measurement, it was possible to attenuate the peaks using an elliptic filter. In the case with two measurements it was not as easy. Instead of improving the loop gain, the elliptic filter made it worse. The magnitude of the controller is shown in Figure 6. The peaks in the amplitude function have the same explanation as for the controller using only q_m . It can be seen that for frequencies above $100 \, \text{rad/s}$, the two \mathcal{H}_{∞} loop shaping controllers behave similar. In the sequel, the controller will be denoted by $\mathcal{H}_{\infty}(q_m, \ddot{\mathcal{P}})$.

V. SIMULATION RESULTS

The three controllers are evaluated using a simulation model. The simulation model consists of the robot model (11), a measurement system, and a controller. The robot model is implemented in continuous-time whereas the controller operates in discrete-time. The continuous-time controllers developed in Section IV, are therefore discretized using Tustin's formula. The measurements are affected by a time delay of one sample as well as zero mean normal

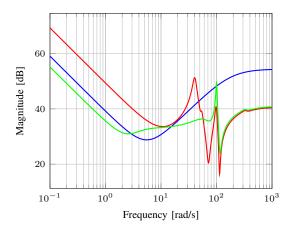


Fig. 6. Controller gain |K| for PID (blue), $\mathcal{H}_\infty(q_m)$ (red), and $\mathcal{H}_\infty(q_m,\ddot{\mathcal{P}})$ (green).

distributed measurement noise. The sample time is $T_s = 0.5 \text{ ms}$.

The system is excited by a disturbance signal w containing steps and a chirp signals on both motor and tool. The nominal performance is evaluated using a performance index, which is a weighted sum of different properties in the simulated tool position and motor torque. The properties for the tool position are the maximum deviations after each step and chirp disturbances as well as settling times after each step disturbances. The properties used in the torque signal is the largest applied torque and the torque noise. The disturbance signal and the performance index are described in more details in [9].

A. Nominal Performance

Nominal performance means that the same model is used both for synthesis of the controllers and in the simulation model. Figure 7 shows how the motor torque differs between the three controllers. It can be seen that $\mathcal{H}_{\infty}(q_m)$ gives a higher torque during the transients, whereas the PID controller gives more noise during steady state. The $\mathcal{H}_{\infty}(q_m, \ddot{\mathcal{P}})$ controller gives the lowest torque changes which implies a lower energy consumption and an increased wear in the motor and gear.

The simulated tool position for the three controllers is shown in Figure 8. For step disturbances, the PID controller deviates more than the other two controllers, and for chirp disturbances the $\mathcal{H}_{\infty}(q_m)$ controller deviates more. The $\mathcal{H}_{\infty}(q_m,\ddot{\mathcal{P}})$ controller deviates the least for both step and chirp disturbances. The response to step disturbances is however slower than for the other two controllers.

The steady state error of approximately 2 mm after 25 s is because of a constant torque disturbance on the tool, which cannot be decreased since the tool position is not measured. The motor position, which is measured for all three controllers, is controlled to zero and due to the flexibilities the tool position cannot be controlled to zero as long as it is not measured.

The performance index V_{nom} for the three controllers is presented in Table I. It shows, as discussed above, that

 $\mathcal{H}_{\infty}(q_m)$ and the PID controller behaves similar and that $\mathcal{H}_{\infty}(q_m, \ddot{\mathcal{P}})$ performs better.

B. Robust Performance

Increasing the time delay by a factor 4 gives a total time delay of $T=2\,\mathrm{ms}$. The performance of the three controllers does not change significantly with the increased time delay, see the performance index V_{delay} in Table I.

When the gain of the system increases by 2.5 more interesting things happen. First of all, the applied motor torque from PID controller oscillates between $^2\pm 20\,\mathrm{Nm}$. The tool position is, in spite of the oscillating motor torque, just a bit worse than in the nominal case. For $\mathcal{H}_{\infty}(q_m)$ and $\mathcal{H}_{\infty}(q_m, \ddot{\mathcal{P}})$ the applied motor torque is decreased by a factor of approximately 2 and the tool position is similar to the nominal case. The reason for a decreased motor torque is that it is not necessary to have the same amount of torque applied on the motor to attenuate a disturbance since the gain of the system from motor torque to output is larger.

The performance index V_{gain} is presented in Table I, where the large value for the PID controller originates from the large torque noise (40 Nm) and the low values for $\mathcal{H}_{\infty}(q_m)$ and $\mathcal{H}_{\infty}(q_m, \ddot{\mathcal{P}})$ originates from the fact that the maximum applied torque is approximately half as much as in the nominal case.

C. Model Order Reduction of K

Model order reduction of the two \mathcal{H}_{∞} controllers will be investigated. For $\mathcal{H}_{\infty}(q_m)$, the Hankel singular values are given by

$$(\infty, 204.56, 189.07, 51.19, 51.15, 48.03, \dots 14.12, 13.07, 3.29, 3.04, 1.98, 1.89, 0.001),$$

from where it can be concluded that a controller of order 6 is sufficient³. Simulations using the reduced order controller have shown no significant degradation of the performance both in the nominal case and when time delay and gain uncertainties are present. The Hankel singular values for $\mathcal{H}_{\infty}(q_m, \ddot{\mathcal{P}})$ are

$$(\infty, 142.85, 139.70, 39.33, 11.84, 11.07, \dots 5.20, 3.13, 2.89, 1.03, 0.01, 0.0005, 0),$$

which indicates that the controller can be reduced to order 6. However, the reduced order controller give an unstable closed loop system. Even a reduction to order 12 gives an unstable closed-loop system.

VI. CONCLUSIONS AND FUTURE WORK

Two different \mathcal{H}_{∞} controllers for a flexible joint of an industrial manipulator are designed using loop shaping. The model, on which the controllers are based, is a four-mass model. As input the controllers use either only the motor angle as input or both the motor angle and the acceleration

²It is the maximum and minimum allowed torque.

 $^{^3}$ The Hankel singular value equal to ∞ corresponds to the integrator in the controller, which is on the stability boundary.

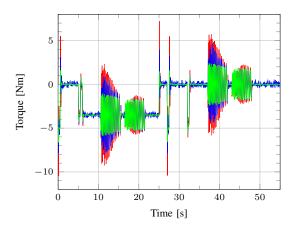


Fig. 7. Motor torque for PID (blue), $\mathcal{H}_{\infty}(q_m)$ (red), and $\mathcal{H}_{\infty}(q_m, \ddot{\mathcal{P}})$ (green).

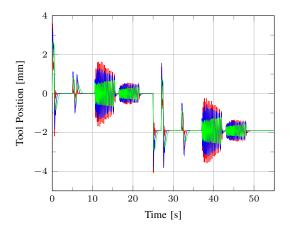


Fig. 8. Tool position for PID (blue), $\mathcal{H}_{\infty}(q_m)$ (red), and $\mathcal{H}_{\infty}(q_m, \ddot{\mathcal{P}})$ (green).

of the end-effector. The controllers are compared to a PID controller and it is shown that there is no significantly improvement using \mathcal{H}_{∞} design methods when only the motor angle is measured. If instead the tool acceleration is added then the performance is improved significantly. However, even with the tool acceleration as a measurement, the steady state error for the tool position is unaffected.

A direct continuation is to investigate the improvement for other types of sensors. One possibility is to have an encoder measuring the position direct after the gearbox, i.e., q_{a1} . It will not eliminate the stationary error for the tool position complete but a decrease in the error can possible be achieved. It is not for practical reasons possible to measure the tool position, instead the tool position can be estimated,

TABLE I

PERFORMANCE INDEX FOR THE THREE CONTROLLERS OPERATING
UNDER NOMINAL CONDITIONS, INCREASE IN TIME DELAY, AND
INCREASE IN SYSTEM GAIN.

	PID	$\mathcal{H}_{\infty}(q_m)$	$\mathcal{H}_{\infty}(q_m, \ddot{\mathcal{P}})$
V_{nom}	55.7	55.4	45.8
V_{qain}	171.5	49.2	29.5
V_{delau}	59.8	56.6	46.0

as described in [1], [2], and used in the feedback loop.

Extending the system to several joints giving a nonlinear model, which has to be linearised in several points, is also a future problem to investigate. A controller is designed in each point and gain scheduling or something similar can be used when the robot moves between different points. Linear parameter varying (LPV) methods are also possible solutions for control of the nonlinear model.

REFERENCES

- Patrik Axelsson. Evaluation of six different sensor fusion methods for an industrial robot using experimental data. In *Proc. of the 10th Int. IFAC Symp. on Robot Contr.*, pages 126–132, Dubrovnik, Croatia, September 2012.
- [2] Patrik Axelsson, Rickard Karlsson, and Mikael Norrlöf. Bayesian state estimation of a flexible industrial robot. Cont. Eng. Pract., 20(11):1220–1228, November 2012.
- [3] Torgny Brogårdh. Present and future robot control development—an industrial perspective. Annual Reviews in Contr., 31(1):69–79, 2007.
- [4] Bram de Jager. The use of acceleration measurements to improve the tracking control of robots. In *Proc. of the IEEE Int. Conf. on Syst.*, *Man, Cybern.*, pages 647–652, Le Touquet, France, October 1993.
- [5] Eric Dumetz, Jean-Yves Dieulot, Pierre-Jean Barre, Frédéric Colas, and Thomas Delplace. Control of an industrial robot using acceleration feedback. J. of Intell. Robot. Sys., 46(2):111–128, 2006.
- [6] Keith Glover and Duncan McFarlane. Robust stabilization of normalized coprime factor plant descriptions with H_∞-bounded uncertainty. *IEEE Trans. Automat. Contr.*, 34(8):821–830, August 1989.
- [7] K. Kosuge, M. Umetsu, and K. Furuta. Robust linearization and control of robot arm using acceleration feedback. In *Proc. of the IEEE Int. Conf. on Contr. and App.*, pages 161–165, Jerusalem, Israel, April 1989.
- [8] Duncan McFarlane and Keith Glover. A loop shaping design procedure using \mathcal{H}_{∞} synthesis. *IEEE Trans. Automat. Contr.*, 37(6):759–769, June 1992.
- [9] Stig Moberg, Jonas Öhr, and Svante Gunnarsson. A benchmark problem for robust feedback control of a flexible manipulator. *IEEE Trans. Contr. Syst. Technol.*, 17(6):1398–1405, November 2009.
- [10] Mark Readman and Pierre Bélanger. Acceleration feedback for flexible joint robots. In *Proc. of the 30th IEEE Conf. on Decision and Contr.*, pages 1385–1390, Brighton, England, December 1991.
- [11] Michael Ruderman and Torsten Bertram. Modeling and observation of hysteresis lost motion in elastic robot joints. In *Proc. of the 10th Int. IFAC Symp. on Robot Contr.*, pages 13–18, Dubrovnik, Croatia, September 2012.
- [12] H. G. Sage, M. F. De Mathelin, and E. Ostertag. Robust control of robot manipulators: A survey. *Int. J. of Contr.*, 72(16):1498–1522, 1999.
- [13] Hansjörg G. Sage, Michel F. de Mathelin, Gabriel Abba, Jacques A. Gangloff, and Eric Ostertag. Nonlinear optimization of robust \mathcal{H}_{∞} controllers for industrial robot manipulators. In *Proc. of the IEEE Int. Conf. on Robot. and Automat.*, pages 2352–2357, Albuquerque, NM, USA, April 1997.
- [14] Sigurd Skogestad and Ian Postletwaite. Multivariable Feedback Control, Analysis and Design. John Wiley & Sons, Chichester, West Sussex, England, second edition, 2005.
- [15] Y. D. Song, A. T. Alouani, and J. N. Anderson. Robust path tracking control of industrial robots: An H_∞ approach. In *Proc. of the IEEE* Conf. on Contr. App., pages 25–30, Dayton, OH, USA, September 1992
- [16] Wayne L. Stout and M. Edwin Sawan. Application of H-infinity theory to robot manipulator control. In *Proc. of the IEEE Conf. on Contr.* App., pages 148–153, Dayton, OH, USA, September 1992.
- [17] W. L. Xu and J. D. Han. Joint acceleration feedback control for robots: Analysis, sensing and experiments. *Robot. and Comp.-Integ. Manufac.*, 16(5):307–320, October 2000.
- [18] Kemin Zhou, John C. Doyle, and Keith Glover. Robust and Optimal Control. Prentice Hall Inc., Upper Saddle River, NJ, USA, 1996.



${\bf Avdelning},\,{\bf Institution}$

Division, Department

Division of Automatic Control Department of Electrical Engineering

D	\mathbf{at}	u	n
ט	aь	u	11

Date

2012-10-26

**A HÖG5*					
Språk Language	Rapporttyp Report category	ISBN			
□ Svenska/Swedish ☑ Engelska/English □	☐ Licentiatavhandling ☐ Examensarbete ☐ C-uppsats ☐ D-uppsats ☑ Övrig rapport ☐	ISRN Serietitel och serienummer Title of series, numbering	ISSN 1400-3902		
URL för elektronisk ver		LiTH-ISY-R-3053			
Titel Single Joint Control of a Flexible Industrial Manipulator using \mathcal{H}_{∞} Loop Shaping Title					
Författare Patrik Axelsson, Anders Helmersson, Mikael Norrlöf Author					
Sammanfattning Abstract		-	-		
	0 111 1 1 1 6 1 1 1				

Control of a flexible joint of an industrial manipulator using \mathcal{H}_{∞} loop shaping design is presented. Two controllers are proposed; 1) \mathcal{H}_{∞} loop shaping using the actuator position, and 2) \mathcal{H}_{∞} loop shaping using the actuator position and the acceleration of end-effector. The two controllers are compared to a standard PID controller where only the actuator position is measured. Using the acceleration of the end-effector improves the nominal performance. The performance of the proposed controllers is not significantly decreased in the case of model error consisting of an increased time delay or a gain error.

Nyckelord

Keywords — Industrial robots, flexible joint, robust control, \mathcal{H}_{∞} loop shaping